Cover Page



Universiteit Leiden



The handle http://hdl.handle.net/1887/138734 holds various files of this Leiden University dissertation.

Author: Hajmohammadebrahimtehrani, K.

Title: Small-molecule inhibitors of bacterial metallo-β-lactamases

Issue Date: 2020-12-16

Chapter 2

Small-molecule aminocarboxylic acids as metallo-β-lactamase inhibitors; Part I.

Parts of this chapter have been published in:

Tehrani, K. H. M. E., Brüchle, N. C., Wade, N., Mashayekhi, V., Pesce, D., van Haren, M., and I. Martin, N. Small molecule carboxylates inhibit metallo- β -lactamases and resensitize carbapenem-resistant bacteria to meropenem. *ACS Infect. Dis.* **6**, 1366–1371.

1. Introduction

Antibiotic resistance threatens to reduce the efficacy of currently available antibiotics and places a substantial burden on global health and the world economy.^{1,2} Resistance to βlactam antibiotics can be caused by a diverse group of enzymes known as β -lactamases. While based on sequence homology these enzymes are categorized in class A-D (known as Ambler classification),³ mechanistically they are classified as serine-β-lactamases (SBLs, Ambler class A, C, and D) or metallo-β-lactamases (MBLs, Ambler class B).⁴ SBLs inactivate β-lactams via the hydrolytic action of a nucleophilic serine in their active site. First-generation SBL inhibitors including clavulanic acid, sulbactam, and tazobactam as well as the more recently approved avibactam and vaborbactam, are available to rescue the antimicrobial activity of β-lactams in the presence of SBL-producing bacteria.^{5,6} MBLs on the other hand are metallo-enzymes that hydrolyze β-lactams by action of a zinc-activated nucleophilic water molecule that is formed in the active site. To date there are no FDA-approved MBL inhibitors available. Of particular concern are the clinically important MBLs including the New Delhi metallo-β-lactamase (NDM), Verona integron-encoded metallo-β-lactamase (VIM), and imipenemase (IMP) families that possess carbapenemase activity, adding further urgency to the development of MBL inhibitors to combat MBL-producing bacterial infections.

Small molecules with the ability to inhibit MBLs have been the topic of a number of comprehensive reviews. $^{8-11}$ The majority of known MBL inhibitors contain functional groups that can bind zinc. In this regard, the most common small molecules possessing anti-MBL activity are thiol-containing compounds, $^{12-15}$ sulfonylhydrazones, 16 bis-carboxylic acids, 17,18 picolinic acids, 19,20 and commonly used chelating agents 21,22 including their bacteria-targeting analogs. 23,24 As an example, the natural product aspergillomarasmine A (AMA), was recently identified by Wright and coworkers who screened fungal extracts for anti-MBL activity. AMA was shown to be a potent inhibitor of both NDM and VIM type enzymes and importantly displays *in vivo* efficacy. 25 Also of interest are the recently developed cyclic boronate SBL- and MBL-inhibitors which mimic the tetrahedral intermediate formed upon nucleophilic attack of a serine-hydroxyl group (SBLs) or zinc-bound water molecule (MBLs) at the β -lactam unit. $^{26-30}$ In addition, recent reports have also described compounds with alternative modes of MBL inhibition including covalent inhibitors $^{31-33}$ and DNA aptamers proposed to operate via allosteric mechanism of inhibition. 34

In reviewing the literature we noted that sulfonic acid buffer components such as MES and PIPES have previously been reported to be weak MBL inhibitors.³⁵ This prompted us to investigate the possibility of identifying new MBL inhibitor candidates among other commonly used small molecule buffer components containing multiple carboxylic acid and/or phosphonate functionalities. Given that zinc binding is a key aspect of the mechanism of action for a majority of MBL inhibitors, we specifically focused our attention on common buffer reagents and structurally related small molecules reported to interact with metals (figure 1).

2. Results and discussion

The panel of small molecules shown in figure 1 were first screened for their inhibitory activity against purified MBLs including NDM-1, VIM-2, and IMP-28. The substrate used for the enzyme inhibition assay was a fluorescent cephalosporin derivative developed by Schofield and co-workers for assessing MBL activity. 36 As shown in table 1, nitrilotriacetic acid (NTA, 3) and its bioisosteres (4 , 5) showed promising activity against NDM-1 and VIM-2 superior to that of dipicolinic acid (DPA), a well-studied MBL inhibitor. 19,20 Notably, the much weaker inhibitory activity of the disubstituted analogs 1 and 2 point to the necessity of three carboxyl(phosphoryl) substituents in order to achieve potent inhibition of NDM-1 and VIM-2, most probably by tightly chelating zinc ions. Interestingly, compounds 1 -8 all exhibited little-to-no activity against IMP-28. This observation is in line with previous investigations that have found the IMP class of MBLs to be less sensitive to inhibition by zinc-binding agents. 25,37 To establish whether the inhibition measured was time-dependent, the IC50 values of compounds 3 , 5 , and DPA for NDM-1 were

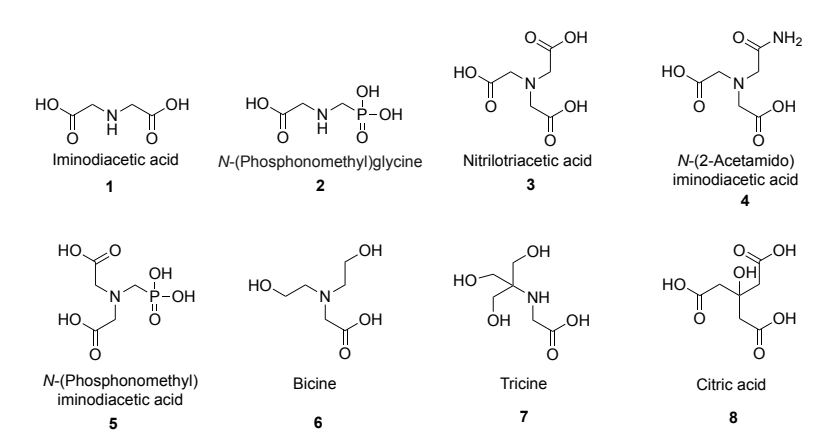


Figure 1. Small-molecule carboxylic acids as potential MBL inhibitors

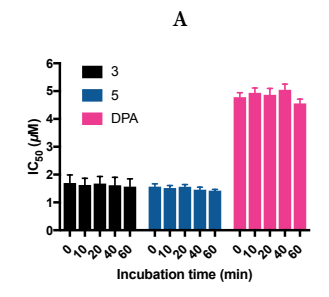
also determined after pre-incubating the inhibitor and enzyme for various times including 0, 10, 20, 40, and 60 minutes as previously described for a different class of NDM-1 inhibitors.³⁸ As shown in figure 2A, pre-incubation time does not significantly affect the potency of the tested compounds under the assay conditions used.

The majority of MBL inhibitors fall into one of two groups: those that interact with zinc as part of their binding in the MBL active site forming a ternary complex, or those that actively strip zinc from the MBL active site driven by their strong chelating ability. 39,40 Captopril is an example of the former while known chelating agents such as EDTA and the fungal secondary metabolite AMA represent the latter. 19,41 In determining the IC50 value of **5** against NDM-1 it was noted that in the presence of different concentrations of zinc sulfate (ranging from 0.1 μ M to 20 μ M), the IC50 values measured also changed revealing a zinc-dependent effect similar to that for DPA. By comparison, and as expected, the inhibitory activity of captopril is not influenced by varying the concentration of exogenous zinc added to the assay media (figure 2B). These findings support a zinc-sequestration based mechanism of NDM-1 inhibition for compound **5**.

Table 1. IC₅₀ values determined against NDM-1, VIM-2, and IMP-28.

11.11 20.							
Compound	$IC_{50} (\mu M)^a$						
	NDM-1	VIM-2	IMP-28				
1	>200	>200	>200				
2	75 ± 2	41 ± 6	>200				
3	1.3 ± 0.07	2.4^{b}	112 ± 3				
4	2.3 ± 0.05	25^{b}	>200				
5	0.91 ± 0.05	0.68 ± 0.02	39 ± 7				
6	>200	>200	>200				
7	>200	>200	>200				
8	132 ± 15	102 ± 7	>200				
DPA	3.8 ± 0.04	2.9 ± 0.5	17 ± 1				

 $^{^{\}alpha}Values$ reported as mean \pm SD of at least 3 independent experiments.



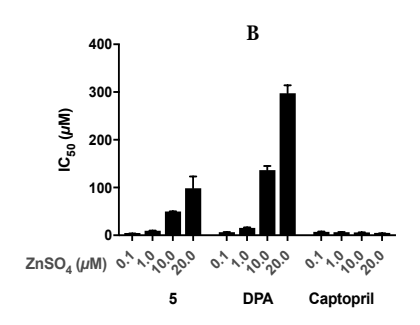


Figure 2. A. The inhibitory activity of compounds **3**, **5**, and DPA over the time-course of 0-60 min against NDM-1. **B.** The effect of zinc on the inhibitory activity of compound **5**, DPA, and captopril against NDM-1.

^bDue to the complex shape of the log[concentration]-activity plot, accurate fitting was not possible, the reported values are therefore an estimation.

Further evidence for high affinity zinc binding by compound **5** was obtained by use of isothermal titration calorimetry (ITC). This technique allows for the direct determination of the dissociation constant (K_d) as well as thermodynamic parameters including ΔG , ΔH , and ΔS . Among the small molecules tested as part of the current study, compounds **3-5** were found to be strong zinc-binders with K_d values of 121 nM, 231 nM, and 56 nM respectively (table 2). Interestingly, the affinity of compounds **3-5** for other biologically-relevant divalent cations like Ca^{2+} and Mg^{2+} was negligible by ITC with binding interactions too weak to allow for an accurate determination of thermodynamic parameters. Previous reports have also described potentiometric titration^{42–44} and ITC based methods for studying the metal binding properties of related compounds. ^{45–47} It should be noted that in these earlier studies, the associated K_d values measured for the binding of Ca^{2+} and Zn^{2+} by DPA were somewhat lower than the values obtained in our investigations, an effect we ascribe to differences in the buffers used. Specifically, given the buffering capacity of the test compounds evaluated in our study, we chose to employ 100 mM Tris buffers to avoid any pH mismatch. Notably, our ITC data reveal a strong correlation between these compounds' capacity to inhibit MBL activity and their zinc binding ability (table 2).

The results of our investigations, as well as other recently published studies, indicate that incorporation of the phosphonic acid moiety is a promising approach in designing potent MBL inhbitors.^{48–50} In line with our findings relating to the enhanced potency of compound **5** relative to compound **3** are recent studies showing that phosphonic acid analogs of picolinic acid demonstrate increased potency against NDM-1.^{20,49} In addition, phosphonate analogs of the well-known mercapto-carboxylic acid MBL inhibitors (represented by thiomandelic acid) demonstrate enhanced inhibitory activity.⁴⁸ In light of our findings and the studies mentioned

Table 2. ITC based thermodynamic parameters for the binding of zinc by compounds **3-5**

Compound		K _d (nM)	ΔH (kcal/mol)	-TΔS (kcal/mol)	ΔG (kcal/mol)
3 a	Zn ²⁺	121 ± 8	-4.89 ± 0.22	-4.55 ± 0.25	-9.40 ± 0.04
4 a	Zn^{2+}	231 ± 10	-2.96 ± 0.07	-6.10 ± 0.08	-9.06 ± 0.03
5^{a}	Zn^{2+}	56 ± 15	-3.08 ± 0.11	-6.84 ± 0.28	-9.91 ±0.16
\mathbf{DPA}^b	Zn^{2+}	2373 ± 367	-2.46 ± 0.18	-5.21 ± 0.27	-7.68 ± 0.09
	Ca ²⁺	34233 ± 525	-5.503 ± 0.05	-0.589 ± 0.05	-6.09 ± 0.01

^aNo appreciable binding to Ca²⁺ and Mg²⁺ was observed.

^bNo appreciable binding to Mg²⁺ was observed.

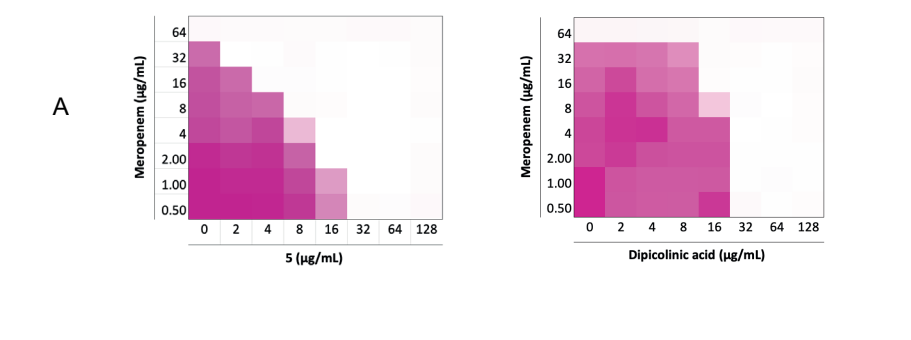
above, incorporation of a phosphonic acid moiety into the structures of other MBL inhibitors such as cyclic boronates (exemplified by VNRX-5133)³⁰ may also provide access to new classes of hybrid MBL inhibitors.

The ability of compounds **1-8** to restore the activity of meropenem, a last resort carbapenem, against a representative MBL-expressing strain was evaluated using a clinical NDM-1 positive isolate (coded *E. coli* RC0089). Using a checkerboard assay, multiple concentration combinations of MBL inhibitor + meropenem where tested allowing for calculation of the fractional inhibitory concentration (FIC) index according to the following expression (where an FIC index of <0.5 indicates a synergistic relationship):

$$FICI = \frac{MIC \text{ of meropenem in combination}}{MIC \text{ of meropenem alone}} + \frac{MIC \text{ of MBL inhibitor in combination}}{MIC \text{ of MBL inhibitor alone}}$$

Among the compounds tested, 3-5 showed a synergistic relationship with meropenem with compound **5** demonstrating the highest potency with the lowest FIC index of 0.047 (figure 3). Compounds 3 and 5 were both very effective in restoring the activity of meropenem against the NDM-1 producing E. coli strain used in the initial screen and were therefore also tested in combination with meropenem against a larger panel of 38 gram-negative clinical isolates displaying carbapenem resistance (table 3). While compounds 3 and 5 exhibited no antibacterial activity at the highest tested concentration of 256 µg/mL, both were found to effectively enhance the activity of meropenem against strains expressing NDM- and VIM-type enzymes. When administered at a concentration of 32 µg/mL both 3 and 5 reduced the MIC of meropenem by up to 128-fold against these strains, a synergism equivalent to or better than that observed for DPA. Overall, compound 5 reduced the MIC of meropenem to its clinically susceptible concentration (≤1 µg/mL) for 67% of the NDM- and VIM-type producing isolates tested while for compound 3 and DPA this ratio was 37% and 53% respectively. By comparison, when tested against strains expressing IMP-type enzymes, the synergistic activity of 3 and 5 was modest, leading to no more than a 4-fold reduction of MIC in most cases, a trend also mirrored for DPA. In addition, the complete lack of synergy observed against strains expressing serine-carbapenemases such as KPC-2 and OXA-48, further demonstrates the inhibitory activities of compounds 3 and 5 to be MBL-specific. Also, among the bacterial species screened, P. aeruginosa proved to be more resistant to the synergistic combinations tested. This is apparent when comparing the

antibacterial activities of the combinations against NDM-1 and VIM-2 producing *P. aeruginosa* isolates versus the corresponding *E. coli* and *K. pneumoniae* counterparts (see table 3).



ъ.	Compound	1	2	3	4	5	6	7	8	DPA
В	Lowest FIC	>0.5	>0.5	0.078	0.266	0.047	>0.5	>0.5	>0.5	0.070

Figure 3. **A**. Checkerboard plots for compound **5** and DPA in combination with meropenem tested against an NDM-1 producing strain of *E. coli*. The optical density of the bacteria at 600 nm (OD₆₀₀) has been shown as color gradient between white (no bacterial growth) and magenta (maximum growth); **B**. The lowest FIC values calculated for compounds **1-8**.

Table 3. MIC of meropenem alone or in combination with compound **3**, **5**, and DPA against a panel of carbapenem-resistant clinical isolates of gram-negative bacteria.

Bacterial isolates	Rlactomosc	MIC (μg/mL)						
	β-lactamase	Mer	$Mer + 3^a$	$Mer + 5^a$	Mer + DPA ^a			
E. coli ^b	NDM-1	8	0.5 (16)	0.125 (64)	0.25 (32)			
E. coli ^b	NDM-1	16	$\leq 0.125 (\geq 128)$	$\leq 0.125 \ (\geq 128)$	0.25 (64)			
E. coli ^c	NDM-1	16	0.5 (32)	0.25 (64)	0.5 (32)			
$E.\ coli^d$	NDM-1	128	4 (32)	0.5 (256)	1 (128)			
K. pneumoniae ^d	NDM-1	32	1 (32)	0.125 (256)	0.5 (64)			
K. pneumoniae ^d	NDM-1	64	4 (16)	≤0.5 (≥128)	1 (64)			
K. pneumoniae ^d	NDM-1	16	1 (16)	0.25 (64)	0.25 (64)			
P. aeruginosa ^e	NDM-1	128	16 (8)	8 (16)	8 (16)			
P. stuartii ^b	NDM-1	32	0.25 (128)	0.25 (128)	0.25 (128)			
A. baumannii ^e	NDM-2	32	4 (8)	2(16)	2 (16)			
$E.\ coli^c$	NDM-4	64	2 (32)	≤0.5 (≥128)	1 (64)			
E. coli ^b	NDM-5	32	4 (8)	0.5 (64)	2 (16)			
$E.\ coli^c$	NDM-5	128	16 (8)	8 (16)	8 (16)			
$E.\ coli^c$	NDM-6	128	32 (4)	8 (16)	8 (16)			
E. coli ^c	NDM-7	32	≤0.5 (≥64)	≤0.5 (≥64)	≤0.5 (≥64)			
E. coli ^c	NDM-15	128	64(2)	32 (4)	64 (2)			
E. aerogenes ^d	VIM-1	16	1 (16)	≤0.25 (≥64)	0.5 (32)			
K. pneumoniae ^b	VIM-1	256	16 (16)	≤2 (≥128)	4 (64)			
K. pneumoniae ^d	VIM-1	32	2 (16)	≤0.5 (≥64)	≤0.5 (≥64)			
K. pneumoniae ^d	VIM-1	256	8 (32)	≤2 (≥128)	4 (64)			
K. pneumoniae ^d	VIM-1	64	≤0.5 (≥128)	≤0.5 (≥128)	≤0.5 (≥128)			
E. coli ^b	VIM-2	8	0.25 (32)	0.125 (64)	0.125 (64)			
K. pneumoniaee	VIM-2	8	0.5 (16)	0.25 (32)	0.25 (32)			
P. aeruginosa ^b	VIM-2	32	8 (4)	4 (8)	4(8)			
P. aeruginosa ^b	VIM-2	16	4 (4)	1(16)	2(8)			
P. aeruginosa ^b	VIM-2	32	2 (16)	2(16)	4(8)			
P. aeruginosa ^d	VIM-2, blapao	16	2 (8)	1(16)	2(8)			
P. aeruginosa ^b	VIM-2, OXA-50, bla _{PAO}	16	2 (8)	1 (16)	2 (8)			
P. aeruginosa ^c	VIM-11	16	2 (8)	1(16)	1(16)			
P. aeruginosa ^c	VIM-28	>256	256 (≥2)	64 (≥8)	128 (≥4)			
P. aeruginosa ^e	IMP-1	>256	256 (≥2)	256 (≥2)	256 (≥2)			
P. aeruginosa ^c	IMP-7	64	16 (4)	16 (4)	16 (4)			
P. aeruginosa ^c	IMP-13	64	32 (2)	16 (4)	16 (4)			
P. aeruginosa ^d	IMP-13, IMP-37, bla _{PAO}	64	32 (2)	16 (4)	16 (4)			
K. pneumoniae ^d	IMP-28	4	0.5 (8)	0.5 (8)	2(2)			
K. pneumoniae ^d	KPC-2	256	256 (1)	256(1)	256 (1)			
K. pneumoniae ^d	OXA-48	32	32 (1)	32 (1)	32 (1)			
E. coli ^f	_	≤0.0625	≤0.0625 (≥1)	≤0.0625 (≥1)	≤0.0625 (≥1)			

 $^{\alpha}$ Each inhibitor was used at 32 μg/mL in combination with meropenem. None of the inhibitors showed toxicity up to 256 μg/mL against the tested strains. Fold reduction of MIC has been shown in brackets. b Source: Vrije Universiteit Medical center, The Netherlands. c Source: The Dutch national institute for public health and the environment. d Source: Utrecht university medical center, The Netherlands. c Source: National reference laboratory for multidrug-resistant gram-negative bacteria, Bochum, Germany. f ATCC 25922, this strain does not harbor any carbapenemase and was used as a negative control.

3. Conclusion

The most clinically relevant MBLs continue to be the NDM, VIM, and IMP classes and present a significant challenge to the efficacy of virtually all classes of β-lactam antibiotics including "last-line-of-defense" carbapenems such as meropenem. Despite this, no inhibitors are clinically available to combat resistant infections caused by gram-negative pathogens that express MBLs. The current study expands our understanding of the diversity of small molecule carboxylic acids that inhibit MBLs and synergize with carbapenems. By screening a series of available and commonly used small-molecule carboxylates, we found that nitrilotriacetic acid (3) and its phosphoric acid analog N-(phosphonomethyl)iminodiacetic acid (5) are both potent inhibitors of NDM- and VIM- type enzymes with sub- to low-uM IC $_{50}$ values. Using ITC both 3 and 5 were shown to bind zinc with nanomolar affinity. When further tested against a broad panel of MBLproducing gram-negative pathogens, compounds 3 and 5 effectively reduced the MIC of meropenem against NDM- and VIM- type enzymes. As for the well-characterized DPA, the mechanism of MBL inhibition for **3** and **5** appears to be largely driven by zinc-sequestration. While such strong zinc-binding compounds are unlikely clinical candidates, they do represent readily available inhibitors for biochemical studies of MBLs. Furthermore, given their small size and structural simplicity, such compounds may serve as leads for further optimization. One approach may be to administer such compounds as prodrugs that are activated only upon entry to the bacterial cell. In the absence of clinically approved MBL-inhibitors, and with increasing rates of MBL-driven carbapenem resistance, it is important that many approaches, including unconventional avenues, be explored in the pursuit of an effective therapeutic response.

4. Experimental section

Enzyme production and purification

For the production of VIM-2 and NDM-1, pOPINF NDM-1 and pTriEx-based pOPINF plasmids (ampicillin resistant) were used. The constructs were a generous gift from Prof. Christopher J. Schofield (Oxford university). In the case of IMP-28, the construct was designed in pET28b with a 6-His tag at the C-terminus. The plasmids of IMP-28, VIM-2, NDM-1 were transformed in BL21 competent E. coli using standard heat shock transformation method. The single colonies were grown overnight at 37 °C in LB medium containing 1% glucose and appropriate antibiotic (100 µg/mL ampicillin or 300 µg/mL amikacin). The cell suspension was diluted 100 times in YT2x supplemented with 0.1% glucose and antibiotic, shaking at 37 °C for about 4 h to reach OD₆₀₀ of 0.5-0.7. The expression of the enzymes was induced by addition of isopropyl β-D-1-thiogalactopyranoside (IPTG, final concentration 0.5 mM). The cells were incubated overnight at 25 °C with shaking and then harvested by centrifugation for 20 min at 6000 rpm. The pellet was resuspended in lysis buffer (PBS, 150 mM NaCl, 0.05% Triton X-100, protease inhibitor cocktail). After two freeze-thaw cycles the cell suspension was incubated with 1 mg/mL lysozyme for 30 min at 37 °C followed by 3 cycles of sonication (30-s pulse and 30-s rest each cycle). The cellular debris were removed by centrifugation at 12000 rpm for 20 min at 4 °C. Äkta Xpress chromatography system was used to purify the enzymes. Briefly, the supernatant was loaded on 1 mL HisTrap HP column and the enzymes were eluted with 300 mM imidazole. The fractions were then loaded on HiTrap desalting column to exchange the buffer. In case of IMP-28, the fractions were collected in 20 mM Tris, 150 mM NaCl, 10% glycerol, 20 µM ZnCl₂. VIM-2 and NDM-1 fractions were buffer exchanged to 20 mM Tris, 200 mM NaCl. The purity of the fractions was determined on 15% SDS-PAGE gel (figure 4). The concertation of the enzymes was measured by Nanodrop at 280 nm. To remove the His tag at the N-termini of VIM-2 and NDM-1, the proteins were incubated overnight at 4 °C with HRV-3C protease (1:100

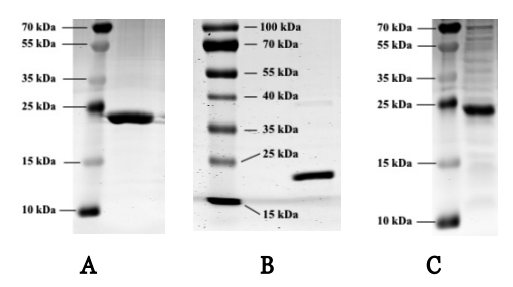


Figure 4. SDS-PAGE gels of purified NDM-1 (A), VIM-2 (B), and IMP-28 (C).

w/w). The digestion mixture was passed through a HisTrap column to separate cleaved from uncleaved enzymes. The cleavage of His tag was confirmed by western blot technique. Both enzymes were buffer exchanged to 50 mM Tris (pH 7.5) containing 500 mM NaCl

IC50 and zinc dependency assay

All the test compounds were dissolved and serially diluted in 50 mM HEPES pH 7.2, supplemented with 0.01% Triton X-100 and 1 μ M ZnSO₄. The MBL enzymes (60 pM NDM-1, 100 pM VIM-2, and 60 pM IMP-28) were then added to the wells and incubated at 25 °C for 15 min. Next, the fluorescent cephalosporin substrate FC5³⁶ (0.5 μ M for NDM-1 and VIM-2, 16 μ M for IMP-28) was added to the wells and fluorescence was monitored immediately over 30-40 scanning cycles (λ_{ex} 380 nm, λ_{em} 460 nm) on a Tecan Spark plate reader. Using the initial velocity data plotted against inhibitor concentration, the half-maximal inhibitory concentrations were calculated by IC₅₀ curve-fitting model in GraphPad Prism 7 software (figure 5). 2,6-Dipicolinic acid was used as positive control. The IC₅₀ of captopril, dipicolinic acid, and **5** was also evaluated in the presence of different concentrations of zinc sulfate (0.1, 1, 10 and 20 μ M) against NDM-1 following the procedure described above.

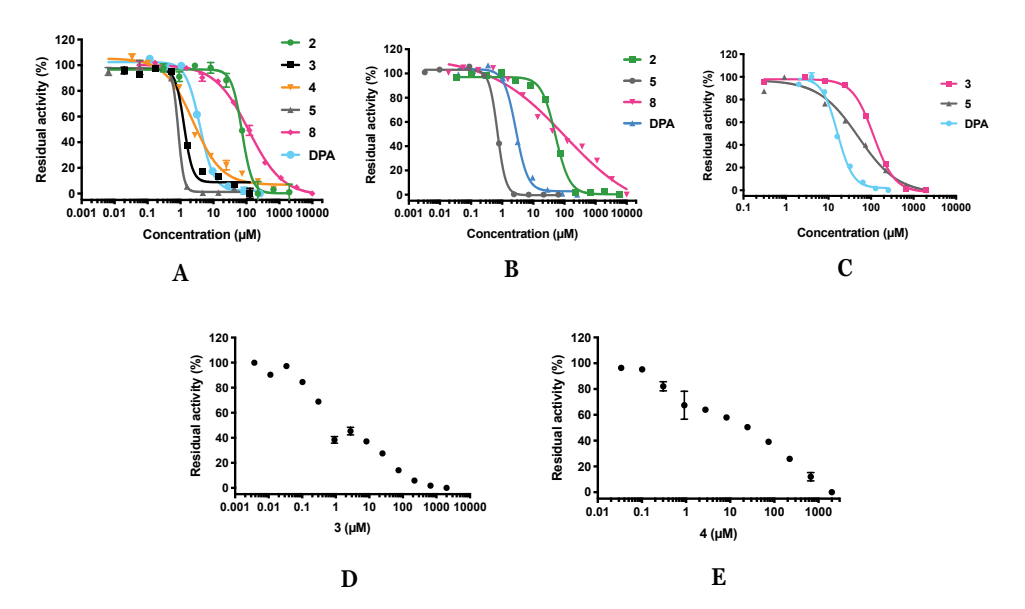


Figure 5. IC₅₀ curves of the test compounds against NDM-1 (**A**), VIM-2 (**B**), and IMP-28 (**C**). The activity plot of compounds **3** (**D**) and **4** (**E**) against VIM-2 did not have a sigmoidal shape.

Isothermal Titration Calorimetry (ITC)

The test compounds were evaluated for their ability to bind zinc using an automated PEAQ-ITC calorimeter (Malvern). Zinc sulfate dissolved in 100 mM Tris (pH 7.0) was titrated into the test compounds dissolved in the same buffer over $19\times2~\mu\text{L}$ aliquots (except for the first aliquot which was $0.4~\mu\text{L}$). The titrations were performed at 25 °C and reference power was set at $10~\mu\text{cal/sec}$. Peak integration and curve-fitting was done using the PEAQ-ITC data analysis software provided by the manufacturer. The blank titrations included buffer titrated in the test compounds, and zinc sulfate titrated in buffer all of which showed negligible signals attributed to heat of dilution (see figure 6 for the thermograms).

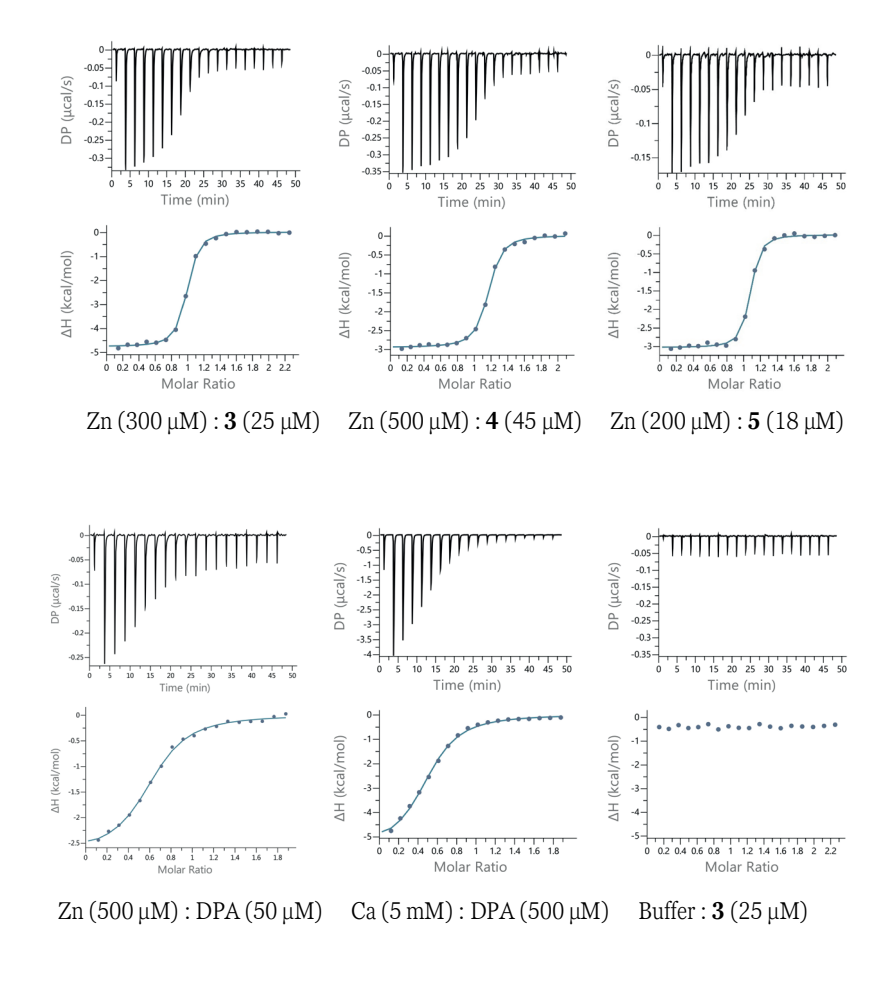


Figure 6. ITC thermograms

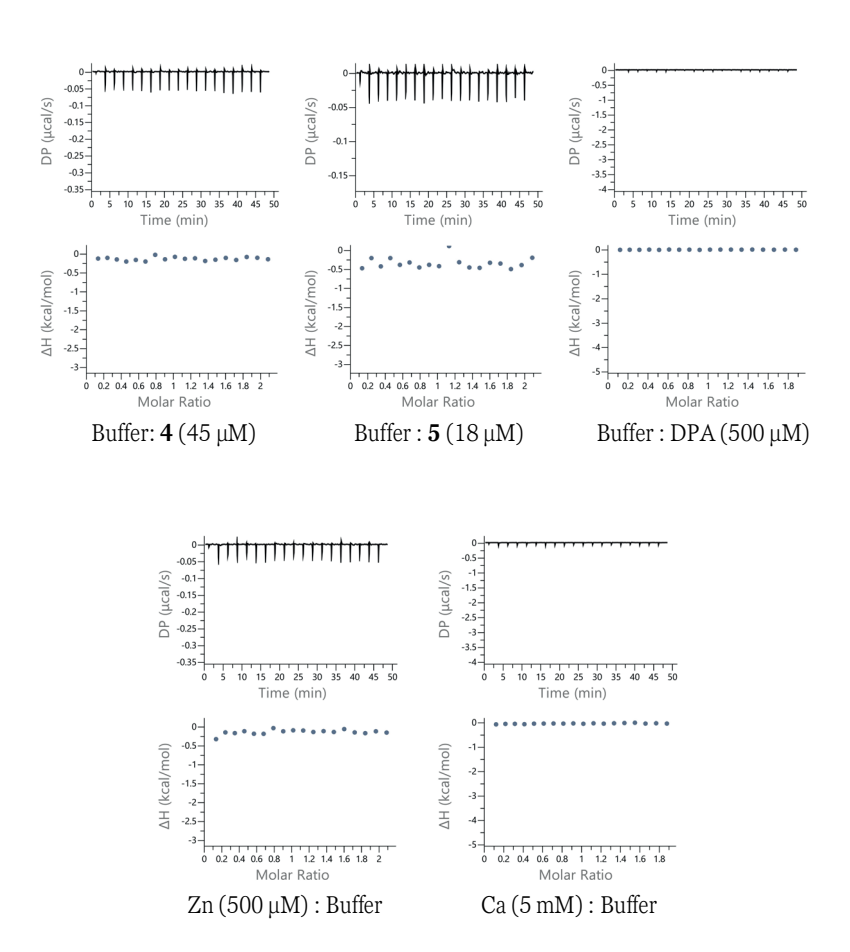


Figure 6. Continued

Antibacterial assays

All antibacterial assays were carried out following the guidelines published by the clinical and laboratory standards institute (CLSI). Bacterial strains and clinical isolates were cultured on blood agar and incubated overnight at 37 °C. Fresh colonies were suspended in tryptic soy broth (TSB) and incubated at 37 °C with shaking. Following growth to exponential phase ($OD_{600} = 0.5$), the bacterial suspension was diluted to 10^6 CFU/mL in Mueller-Hinton broth (MHB) and added to the test compounds prepared as described for each assay:

A. Single concentration synergy assay. On a polypropylene microplate, meropenem was dissolved and serially diluted in MHB (25 μ L/well). Compounds **3**, **5**, and DPA with the final concentration of 32 μ g/mL (25 μ L/well) were then added to the wells. Following the addition of the diluted bacterial suspensions prepared as described above (50 μ L/well), the microplates were incubated at 37 °C with shaking and after 16-20 h, the plates were inspected for the bacterial growth. Minimum inhibitory concentration (MIC) values were reported as the lowest concentration of the antibiotic/test compounds that prevents the visible growth of bacteria. All the assays were performed in triplicate and the median values were used to report MICs.

B. OD_{600} checkerboard assay. Meropenem was dissolved and serially diluted on the polypropylene microplates in MHB (25 μ L/well). The test compounds dissolved and serially diluted to the final concentration ranging from 128 μ g/mL to 1 μ g/mL were then added to meropenem (25 μ L/well). *E. coli* RC0089, a clinical isolate producing NDM-1, grown to the exponential phase and diluted in MHB was added to the microplate (50 μ L/well) which was then incubated at 37 °C with shaking. After 16-20 h, the optical density of wells was scanned at 600 nm on a Tecan Spark plate reader (figure 7).

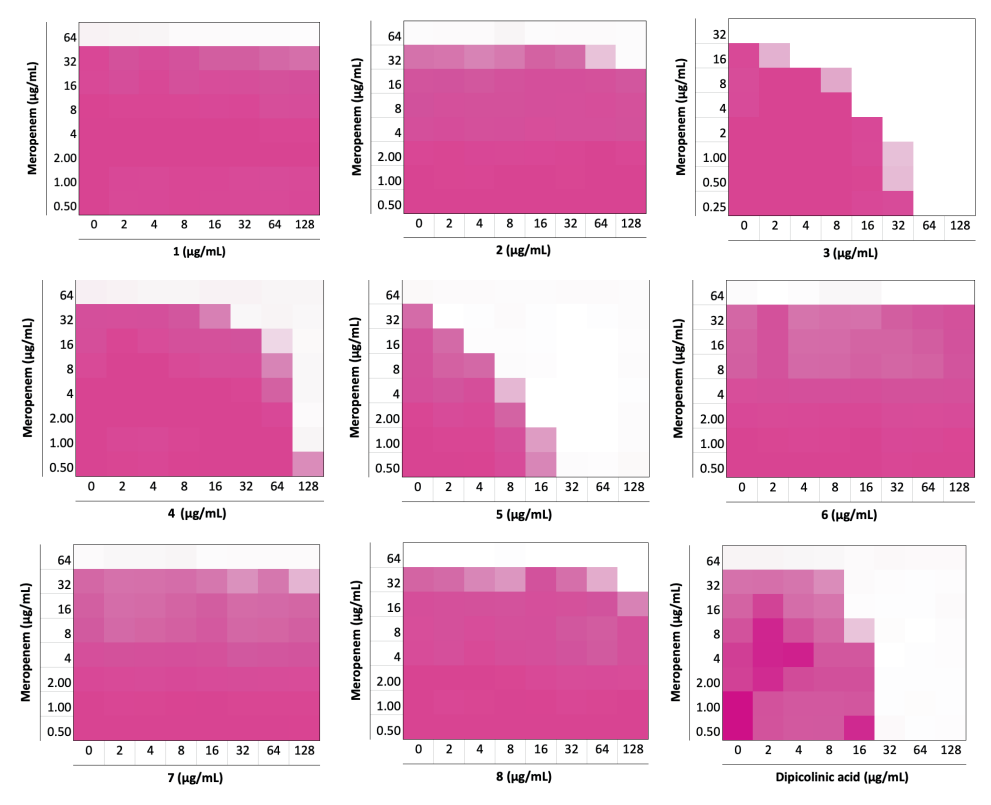


Figure 7. Checkerboard assays of the tested small molecules in combination with meropenem against an NDM-1 producing clinical isolate of *E. coli*. The optical density of the bacteria at 600 nm (OD₆₀₀) has been shown as color gradient between white (no bacterial growth) and magenta (maximum growth).

Acknowledgements

The enzyme experiments were made possible thanks to the contributions of Diego Pesce to design the plasmid construct of IMP-28, Vida Mashayekhi to express and purify NDM-1, VIM-2, and IMP-28, and Matthijs van Haren to synthesize the FC5 substrate.

References

- 1 M. Ferri, E. Ranucci, P. Romagnoli and V. Giaccone, *Crit. Rev. Food Sci. Nutr.*, 2017, 57, 2857–2876.
- B. Aslam, W. Wang, M. I. Arshad, M. Khurshid, S. Muzammil, M. H. Rasool, M. A. Nisar, R. F. Alvi, M. A. Aslam, M. U. Qamar, M. K. F. Salamat and Z. Baloch, *Infect. Drug Resist.*, 2018, **2018**, 1645–1658.
- 3 R. P. Ambler, *Philos. Trans. R. Soc. Lond. B. Biol. Sci.*, 1980, **289**, 321–331.
- 4 S. M. Drawz and R. A. Bonomo, *Clin. Microbiol. Rev.*, 2010, **23**, 160–201.
- 5 K. H. M. E. Tehrani and N. I. Martin, *Medchemcomm*, 2018, **9**, 1439–1456.
- 6 K. Bush, ACS Infect. Dis., 2018, 4, 84–87.
- 7 M. F. Mojica and R. A. B. and W. Fast, Curr. Drug Targets, 2016, 17, 1029–1050.
- 8 W. Fast and L. D. Sutton, *Biochim. Biophys. Acta Proteins Proteomics*, 2013, **1834**, 1648–1659.
- 9 P. W. Groundwater, S. Xu, F. Lai, L. Váradi, J. Tan, J. D. Perry and D. E. Hibbs, *Future Med. Chem.*, 2016, **8**, 993–1012.
- 10 R. P. McGeary, D. T. Tan and G. Schenk, *Future Med. Chem.*, 2017, **9**, 673–691.
- P. Linciano, L. Cendron, E. Gianquinto, F. Spyrakis and D. Tondi, *ACS Infect. Dis.*, 2019, **5**, 9–34.
- 12 C. Mollard, C. Moali, C. Papamicael, C. Damblon, S. Vessilier, G. Amicosante, C. J. Schofield, M. Galleni, J. M. Frère and G. C. K. Roberts, J. Biol. Chem., 2001, 276, 45015–45023.
- 13 K. H. M. E. Tehrani and N. I. Martin, *ACS Infect. Dis.*, 2017, **3**, 711–717.
- D. Büttner, J. S. Kramer, F.-M. Klingler, S. K. Wittmann, M. R. Hartmann, C. G. Kurz,
 D. Kohnhäuser, L. Weizel, A. Brüggerhoff, D. Frank, D. Steinhilber, T. A. Wichelhaus,
 D. Pogoryelov and E. Proschak, ACS Infect. Dis., 2018, 4, 360–372.
- Z. Meng, M.-L. Tang, L. Yu, Y. Liang, J. Han, C. Zhang, F. Hu, J.-M. Yu and X. Sun, ACS Infect. Dis., 2019, 5, 903–916.
- S. Siemann, D. P. Evanoff, L. Marrone, A. J. Clarke, T. Viswanatha and G. I. Dmitrienko, *Antimicrob. Agents Chemother.*, 2002, **46**, 2450–2457.
- 17 L. Feng, K.-W. Yang, L.-S. Zhou, J.-M. Xiao, X. Yang, L. Zhai, Y.-L. Zhang and M. W. Crowder, *Bioorg. Med. Chem. Lett.*, 2012, **22**, 5185–5189.
- 18 Y. Hiraiwa, J. Saito, T. Watanabe, M. Yamada, A. Morinaka, T. Fukushima and T. Kudo, *Bioorg. Med. Chem. Lett.*, 2014, **24**, 4891–4894.

- A. Y. Chen, P. W. Thomas, A. C. Stewart, A. Bergstrom, Z. Cheng, C. Miller, C. R. Bethel,
 S. H. Marshall, C. V Credille, C. L. Riley, R. C. Page, R. A. Bonomo, M. W. Crowder, D.
 L. Tierney, W. Fast and S. M. Cohen, J. Med. Chem., 2017, 60, 7267–7283.
- 20 A. Y. Chen, P. W. Thomas, Z. Cheng, N. Y. Xu, D. L. Tierney, M. W. Crowder, W. Fast and S. M. Cohen, *ChemMedChem*, 2019, **14**, 1271–1282.
- A. M. Somboro, D. Tiwari, L. A. Bester, R. Parboosing, L. Chonco, H. G. Kruger, P. I. Arvidsson, T. Govender, T. Naicker and S. Y. Essack, *J. Antimicrob. Chemother.*, 2015, **70**, 1594–1596.
- 22 R. Azumah, J. Dutta, A. M. Somboro, M. Ramtahal, L. Chonco, R. Parboosing, L. A. Bester, H. G. Kruger, T. Naicker, S. Y. Essack and T. Govender, *J. Appl. Microbiol.*, 2016, **120**, 860–867.
- V. Yarlagadda, P. Sarkar, S. Samaddar, G. B. Manjunath, S. Das Mitra, K. Paramanandham, B. R. Shome and J. Haldar, *ACS Infect. Dis.*, 2018, **4**, 1093–1101.
- C. Schnaars, G. Kildahl-Andersen, A. Prandina, R. Popal, S. Radix, M. Le Borgne, T. Gjøen, A. M. S. Andresen, A. Heikal, O. A. Økstad, C. Fröhlich, Ø. Samuelsen, S. Lauksund, L. P. Jordheim, P. Rongved and O. A. H. Åstrand, ACS Infect. Dis., 2018, 4, 1407–1422.
- A. M. King, S. A. Reid-Yu, W. Wang, D. T. King, G. De Pascale, N. C. Strynadka, T. R. Walsh, B. K. Coombes and G. D. Wright, *Nature*, 2014, **510**, 503–506.
- 26 A. Krajnc, P. A. Lang, T. D. Panduwawala, J. Brem and C. J. Schofield, *Curr. Opin. Chem. Biol.*, 2019, **50**, 101–110.
- S. T. Cahill, J. M. Tyrrell, I. H. Navratilova, K. Calvopiña, S. W. Robinson, C. T. Lohans, M. A. McDonough, R. Cain, C. W. G. Fishwick, M. B. Avison, T. R. Walsh, C. J. Schofield and J. Brem, *Biochim. Biophys. Acta Gen. Subj.*, 2019, **1863**, 742–748.
- G. W. Langley, R. Cain, J. M. Tyrrell, P. Hinchliffe, K. Calvopiña, C. L. Tooke, E. Widlake, C. G. Dowson, J. Spencer, T. R. Walsh, C. J. Schofield and J. Brem, *Bioorg. Med. Chem. Lett.*, 2019, 29, 1981–1984.
- A. Krajnc, J. Brem, P. Hinchliffe, K. Calvopiña, T. D. Panduwawala, P. A. Lang, J. J. A. G. Kamps, J. M. Tyrrell, E. Widlake, B. G. Saward, T. R. Walsh, J. Spencer and C. J. Schofield, *J. Med. Chem.*, 2019, **62**, 8544–8556.
- 30 B. Liu, R. E. L. Trout, G.-H. Chu, D. McGarry, R. W. Jackson, J. C. Hamrick, D. M. Daigle, S. M. Cusick, C. Pozzi, F. De Luca, M. Benvenuti, S. Mangani, J.-D. Docquier, W. J. Weiss, D. C. Pevear, L. Xerri and C. J. Burns, *J. Med. Chem.*, 2020, **6**, 2789–2801.

- 31 P. W. Thomas, M. Cammarata, J. S. Brodbelt and W. Fast, *ChemBioChem*, 2014, **15**, 2541–2548.
- 32 J. Chiou, S. Wan, K.-F. Chan, P.-K. So, D. He, E. W. Chan, T. Chan, K. Wong, J. Tao and S. Chen, *Chem. Commun.*, 2015, **51**, 9543–9546.
- 33 T. Christopeit, A. Albert and H.-K. S. Leiros, Bioorg. Med. Chem., 2016, 24, 2947–2953.
- 34 N. H. Khan, A. A. Bui, Y. Xiao, R. B. Sutton, R. W. Shaw, B. J. Wylie and M. P. Latham, *PLoS One*, 2019, **14**, e0214440.
- 35 P. M. D. Fitzgerald, J. K. Wu and J. H. Toney, *Biochemistry*, 1998, **37**, 6791–6800.
- 36 S. S. van Berkel, J. Brem, A. M. Rydzik, R. Salimraj, R. Cain, A. Verma, R. J. Owens, C. W. G. Fishwick, J. Spencer and C. J. Schofield, *J. Med. Chem.*, 2013, **56**, 6945–6953.
- A. Proschak, J. Kramer, E. Proschak and T. A. Wichelhaus, *J. Antimicrob. Chemother.*, 2017, **73**, 425–430.
- 38 S. T. Cahill, R. Cain, D. Y. Wang, C. T. Lohans, D. W. Wareham, H. P. Oswin, J. Mohammed, J. Spencer, C. W. G. Fishwick, M. A. McDonough, C. J. Schofield and J. Brem, *Antimicrob. Agents Chemother.*, 2017, **61**, e02260-16.
- 39 L. C. Ju, Z. Cheng, W. Fast, R. A. Bonomo and M. W. Crowder, *Trends Pharmacol. Sci.*, 2018, **39**, 635–647.
- 40 C. M. Rotondo and G. D. Wright, *Curr. Opin. Microbiol.*, 2017, **39**, 96–105.
- A. Bergstrom, A. Katko, Z. Adkins, J. Hill, Z. Cheng, M. Burnett, H. Yang, M. Aitha, M. R. Mehaffey, J. S. Brodbelt, K. H. M. E. Tehrani, N. I. Martin, R. A. Bonomo, R. C. Page, D. L. Tierney, W. Fast, G. D. Wright and M. W. Crowder, *ACS Infect. Dis.*, 2018, **4**, 135–145.
- 42 L. Chung, K. S. Rajan, E. Merdinger and N. Grecz, *Biophys. J.*, 1971, **11**, 469–482.
- 43 H. A. Azab, Z. M. Anwar and M. Sokar, *J. Chem. Eng. Data*, 2004, **49**, 62–72.
- 44 C. R. Krishnamoorthy and R. Nakon, *J. Coord. Chem.*, 1991, **23**, 233–243.
- D. Wyrzykowski, B. Pilarski, D. Jacewicz and L. Chmurzyński, *J. Therm. Anal. Calorim.*, 2013, **111**, 1829–1836.
- D. Wyrzykowski, A. Tesmar, D. Jacewicz, J. Pranczk and L. Chmurzyński, *J. Mol. Recognit.*, 2014, **27**, 722–726.
- 47 A. Tesmar, D. Wyrzykowski, E. Muñoz, B. Pilarski, J. Pranczk, D. Jacewicz and L. Chmurzyński, *J. Mol. Recognit.*, 2017, **30**, e2589.
- 48 P. Lassaux, M. Hamel, M. Gulea, H. Delbrück, P. S. Mercuri, L. Horsfall, D. Dehareng,

- M. Kupper, J.-M. Frère, K. Hoffmann, M. Galleni and C. Bebrone, *J. Med. Chem.*, 2010, **53**, 4862–4876.
- 49 P. Hinchliffe, C. A. Tanner, A. P. Krismanich, G. Labbé, V. J. Goodfellow, L. Marrone,
 A. Y. Desoky, K. Calvopiña, E. E. Whittle, F. Zeng, M. B. Avison, N. C. Bols, S. Siemann,
 J. Spencer and G. I. Dmitrienko, *Biochemistry*, 2018, 57, 1880–1892.
- O. A. Pemberton, P. Jaishankar, A. Akhtar, J. L. Adams, L. N. Shaw, A. R. Renslo and
 Y. Chen, *J. Med. Chem.*, 2019, 62, 8480–8496.